

# The story of Seyfert galaxy RE J2248–511: from intriguingly ultrasoft to unremarkably average

R. L. C. Starling,<sup>1★</sup> C. Done,<sup>2</sup> C. Jin,<sup>2</sup> E. Romero-Colmenero,<sup>3</sup> S. B. Potter,<sup>3</sup>  
K. Wiersema,<sup>1</sup> K. L. Page,<sup>1</sup> M. J. Page,<sup>4</sup> A. A. Breeveld<sup>4</sup> and A. P. Lobban<sup>1</sup>

<sup>1</sup>Department of Physics and Astronomy, University of Leicester, University Road, Leicester LE1 7RH, UK

<sup>2</sup>Department of Physics, University of Durham, South Road, Durham DH1 3LE, UK

<sup>3</sup>South African Astronomical Observatory, PO Box 9, Observatory 7935, Cape Town, South Africa

<sup>4</sup>Mullard Space Science Laboratory, University College London, Holmbury St. Mary, Dorking, Surrey RH5 6NT, UK

Accepted 2013 November 9. Received 2013 October 16; in original form 2013 August 25

## ABSTRACT

RE J2248–511 is one of only 14 non-blazar active galactic nuclei (AGN) detected in the far-ultraviolet (FUV) by the *ROSAT* Wide Field Camera implying a large ultrasoft X-ray flux. This soft X-ray excess is strongly variable on year time-scales, a common property of narrow-line Seyfert 1s, yet its optical line widths classify this source as a broad-lined Seyfert 1 (BLS1). We use four nearly simultaneous optical–X-ray spectral energy distributions (SEDs) spanning 7 yr to study the spectral shape and long-term variability of RE J2248–511. Here we show that the continuum SED for the brightest epoch data set is consistent with the mean SED of a standard quasar, and matches well to that from an *XMM*–Sloan Digital Sky Survey sample of AGN with  $\langle M/M_{\odot} \rangle \sim 10^8$  and  $\langle L/L_{\text{Edd}} \rangle \sim 0.2$ . All the correlated optical and soft X-ray variability can be due entirely to a major absorption event. The only remarkable aspect of this AGN is that there is no measurable intrinsic X-ray absorption column in the brightest epoch data set. The observed FUV flux is determined by the combination of this and the fact that the source lies within a local absorption ‘hole’. RE J2248–511, whose variable, ultrasoft X-ray flux once challenged its BLS1 classification, demonstrates that characterization of such objects requires multi-epoch, multiwavelength campaigns.

**Key words:** galaxies: individual: RE J2248-511 – galaxies: Seyfert.

## 1 INTRODUCTION

The ultraviolet (UV) to X-ray spectral shapes seen in active galactic nuclei (AGN) clearly comprise multiple components and have been the subject of decades of study. There is an accretion disc, which peaks in the UV (forming the big blue bump) in the standard optically thick, geometrically thin disc solutions (Shakura & Sunyaev 1973). This emission forms the seed photons for Compton upscattering in a hot corona, producing a power law above 2 keV. However, an excess of soft (<2 keV) X-ray emission above this power-law emission is seen ubiquitously in all high mass accretion rate AGN. The origin of this soft X-ray excess component is currently unknown but if this represents a true additional continuum (e.g. Laor et al. 1997; Magdziarz et al. 1998; Gierliński & Done 2004), then it has very similar temperature in all sources (Czerny et al. 2003; Gierliński & Done 2004; Middleton, Done & Gierliński 2007). This apparent fine tuning led to alternative models where the soft excess

instead arises via reflection/absorption from partially ionized material, so that atomic features set the fixed energy (Gierliński & Done 2004; Crummy et al. 2006; Middleton et al. 2007; Walton et al. 2013). However, both these scenarios predict strong atomic features, at odds with the observed smooth soft X-ray excess continuum. These features can be smoothed into a pseudo-continuum by strong velocity shear, but the velocities required appear too extreme to be plausible for an absorbing wind (Schurch & Done 2007), and even in reflection require the very innermost edge of the disc around a high spin black hole (Crummy et al. 2006; Walton et al. 2013). Reflection also has the problem that the ionization state must be fine-tuned (Done & Nayakshin 2007), resurrecting the very issue that the model was designed to avoid.

The narrow-line Seyfert 1 (NLS1) subclass, objects where the full width at half-maximum (FWHM) of the broad component of the H $\beta$  line is  $\leq 2000$  km s<sup>-1</sup> (Osterbrock & Pogge 1985), shows nearly ubiquitous strong, steep soft X-ray emission (Boller, Brandt & Fink 1996; Grupe et al. 1999). These are most probably low-mass black holes accreting at high mass accretion rates with respect to Eddington ( $L/L_{\text{Edd}} \sim 1$ ; Boroson 2002), so much of the soft

★E-mail: rlcsl@star.le.ac.uk

excess may well be due to intrinsic emission from the accretion disc (Done et al. 2012, hereafter D12; Jin et al. 2012a, hereafter J12a). The combination of low mass and high  $L/L_{\text{Edd}}$  predicts that the NLS1 should have the highest intrinsic accretion disc temperature of all AGN, and that this can peak close to (or even in) the soft X-ray bandpass. These objects do still need an additional soft X-ray component ‘filling in’ smoothly between the disc and high energy power law, but this ‘true’ soft X-ray excess is a much smaller fraction of the inferred bolometric luminosity than in standard broad-line Seyfert 1’s (BLS1; D12; J12a).

A subset of NLS1 also shows dramatic variability, with deep dips in X-ray flux. These dip spectra are extremely complex (Gallo 2006), but can be fit with extremely smeared relativistic reflection (e.g. Fabian et al. 2009, 2013). However, the NLS1 which does not show such dips tend to have rather simple spectra (see Jin et al. 2009, J12a; Middleton et al. 2009; Jin, Ward & Done 2012c). In these ‘simple’ sources, the fast variability strongly favours the original model of a separate soft X-ray Comptonization component (Jin et al. 2013). Standard broad-line Seyferts also show growing evidence from variability studies for a separate soft X-ray component (e.g. Mehdipour et al. 2011; Noda et al. 2011, 2013; Lohfink et al. 2013). While the fine-tuning of the temperature is still an issue, such a component could arise from shock heating of the disc surface from the impact of a failed wind (Done et al. 2013).

Many AGN samples have been studied through their spectral energy distributions (SEDs), facilitated by large extragalactic surveys undertaken with e.g. *XMM-Newton*, *Chandra* and the Sloan Digital Sky Survey (SDSS) and by the availability of simultaneous optical to X-ray data sets from *XMM-Newton* and *Swift* which avoid any confusion introduced by variability (e.g. Brocksopp et al. 2006; Vasudevan & Fabian 2009; Grupe et al. 2010). While this has highlighted the diversity in broad-band spectral shapes and their variability, it has also been possible to create mean spectra for particular classes (e.g. Elvis et al. 1994; J12a). A number of SED studies have concluded that Eddington ratio is a main driver for the SED shape (e.g. Vasudevan & Fabian 2007, 2009; J12a). If this is true then the physics responsible for the soft X-ray excesses in NLS1 is likely to be closely tied to the Eddington ratio. Hence defining this class of objects on a single line width measure would then be inappropriate, missing higher mass black holes at similarly high  $L/L_{\text{Edd}}$  (Sulentic, Marziani & Dultzin-Hacyan 2000; Collin et al. 2006; Dultzin et al. 2011; Peterson 2011). However, high mass, high  $L/L_{\text{Edd}}$  AGN are rare in the local Universe, predominantly due to downsizing of activity in the Universe from  $z \sim 2$ , so the single line width criterion may not miss many local objects.

RE J2248–511 is a local ( $z \sim 0.1$ ), extreme-UV (EUV)-selected Seyfert galaxy. It is classified as a BLS1 due to its Balmer broad-line widths of FWHM  $\sim 3600 \text{ km s}^{-1}$ . For an estimated black hole mass of  $\sim 10^8 M_{\odot}$ , this source is highly variable in both optical and soft X-rays (Puchnarewicz et al. 1995; Breeveld, Puchnarewicz & Otani 2001). *ROSAT* measured a soft X-ray spectral slope of  $\Gamma \sim 3$  and it was among the tiny fraction of *ROSAT* All Sky Survey (RASS) AGN also detected, and in this case discovered, by the *ROSAT* Wide Field Camera in the far-ultraviolet (Pounds et al. 1993). Despite its soft X-ray slope, there is no evidence for strong Fe II emission (e.g. Wilkes, Elvis & McHardy 1987; Boller, Brandt & Fink 1996). This curious mixture of properties often places RE J2248–511 in the crossover of parameter space between BLS1 and NLS1.

RE J2248–511 is then an object where we can examine the nature of the soft X-ray excess and the relationship between the X-ray and optical/UV continua. To probe the underlying physics of this AGN we have gathered four epochs of quasi-simultaneous optical and

X-ray observations using the South African Astronomical Observatory (SAAO) 1.9-m Radcliffe telescope, the Danish 1.54-m telescope at La Silla, *XMM-Newton* and *Swift*, spanning 7 yr from 2000 October to 2007 September. We also make a comparison to archival data. Section 2 describes the observations and in Section 3 we confirm the broad-line cloud velocities and estimate the black hole mass from our optical spectroscopy. We then determine whether the SEDs can be well represented by the broad-band spectral models of D12 in Section 4, and evaluate spectral variability between epochs. We discuss our findings and conclude in Section 5.

## 2 OBSERVATIONS

### 2.1 X-ray

RE J2248–511 was observed with *XMM-Newton* (Jansen et al. 2001) on 2000 October 26 (observations 0109 070 401 and 0109 070 501), 2000 October 31 (0109 070 601) and 2007 May 15 (0510 380 101) as listed in Table 1. We do not use observation 0109 070 501 due to sustained background flaring. All European Photon Imaging Camera (EPIC; Strüder et al. 2001) instruments were in small window mode with the medium filter applied, excepting the MOS cameras during the 2000 observation which were then in small window free running mode. The raw data were processed with the *XMM SAS* version 20110223\_1801-11.0.0.

The source was observed with the X-Ray Telescope (XRT; Burrows et al. 2005) on board *Swift* (Gehrels et al. 2004) on 2006 September 21–22, 2006 November 1 and on 2007 September 15 and 26 (Table 1). We obtained the extracted spectra from the UK Swift Science Data Centre,<sup>1</sup> combining the two 2007 observations into a single spectrum following the procedures of Evans et al. (2009). Data were processed with the *Swift* software version 3.9 using CALDB 3.9.

All X-ray spectra were grouped such that a minimum of 20 counts fell in each bin, and we used the energy range 0.3–10 keV for analysis of *XMM-Newton* and *Swift* X-ray spectra.

### 2.2 Optical

A bright star ( $\epsilon$  Gru with  $V \sim 3.5$ ) is located close ( $\sim 9.1$  arcmin) to the AGN, which made observations with the *XMM-Newton* Optical Monitor and the *Swift* UV Optical Telescope impossible. Observations were, however, possible with ground-based telescopes, listed in Table 1.

RE J2248–511 was observed on 2000 October 19–24, 2001 October 15 and 2007 May 16 using the SAAO 1.9-m Radcliffe telescope with the grating spectrograph and SITE CCD. These observations coincide with the *XMM-Newton* observations to within 2–6 d in 2000, 2.5 weeks in 2001 and 2 d in 2007. Spectra were taken using both a narrow slit ( $\sim 1.8$  arcsec) and a much wider slit, with overlapping blue (#7) and red (#8) gratings ( $\lambda_{\text{central}} = 4600, 7800 \text{ \AA}$ ) in 2000 and 2007. Only the blue grating was used in 2001. Exposure times ranged from 500 to 900 s per spectrum. Arc spectra were taken before and after every target and every standard spectrum using a CuAr lamp. The standard star LTT 9239 was observed for flux calibration of RE J2248–511. Spectra were reduced using standard tools within IRAF. In 2000 spectra were obtained on three separate nights and under variable weather conditions, during which no appreciable variability is seen. For continuum measurement and SEDs

<sup>1</sup> [www.swift.ac.uk/user\\_objects](http://www.swift.ac.uk/user_objects)

**Table 1.** UV, optical and X-ray observations utilized in this work.

Waveband	Obs. date	Telescope and instrument	$T_{\text{exp}}$ (s)	Reference
X-ray	2007 September 26	<i>Swift</i> XRT	1919	Grupe et al. (2010)
	2007 September 15	<i>Swift</i> XRT	22 569	Grupe et al. (2010)
	2007 May 15–16	<i>XMM-Newton</i> EPIC pn	45 058	Dunn et al. (2010)
	2007 May 15	<i>XMM-Newton</i> EPIC MOS 1, 2	57 579, 58 848	Dunn et al. (2010)
	2006 November 01	<i>Swift</i> XRT	5769	Grupe et al. (2010)
	2006 September 21–22	<i>Swift</i> XRT	9759	Grupe et al. (2010)
	2001 October 31	<i>XMM-Newton</i> EPIC pn	9767	
	2001 October 31	<i>XMM-Newton</i> EPIC MOS 1, 2	14 301, 14 304	
	2000 October 26	<i>XMM-Newton</i> EPIC pn	10 089	
	2000 October 26	<i>XMM-Newton</i> EPIC MOS 1, 2	13 789, 13 791	
	1997 May 17	ASCA GIS2, GIS3	19 960, 19 956	Breeveld et al. (2001)
	1993 April 21	ROSAT PSPC	4520	Pounds et al. (1993), Puchnarewicz et al. (1995)
	UV	2004 July 07	<i>FUSE</i>	3299
2002 September 24		<i>FUSE</i>	5534	Dunn et al. (2010)
2002 September 24		<i>FUSE</i>	31 301	Dunn et al. (2010)
1992 November 23		<i>IUE</i> SWP	10 799.8	Dunn et al. (2006)
Optical	2007 May 16	SAAO 1.9 m (low-res blue, red)	900	
	2006 August 29	Danish 1.54 m DFOSC <i>B</i> , <i>V</i> , <i>R</i>	180, 2 × 120, 60	
	2001 October 15	SAAO 1.9 m (blue grating)	900	
	2000 October 19–20	SAAO 1.9 m (low-res blue, red)	500, 500	
	2000 October 19–20	SAAO 1.9 m (high-res blue, red)	500, 500	
	2000 October 21–22	SAAO 1.9 m (low-res blue, red)	600, 900	
	2000 October 21–22	SAAO 1.9 m (high-res blue, red)	600, 600	
	2000 October 23–24	SAAO 1.9 m (low-res blue, red)	600, 900	
	2000 October 23–24	SAAO 1.9 m (high-res blue, red)	600, 600	

in 2000 October we use the spectra on 21st–22nd which were taken under the best seeing conditions. We use the wide-slit data for SED modelling and the narrow-slit data for spectral line measurements.

We observed RE J2248–511 on 2006 August 29 with the Danish 1.5-m telescope at La Silla, using the Danish Faint Object Spectrograph and Camera (DFOSC) instrument for optical photometry. These observations lie within 3 weeks of the first *Swift* pointing. The following filters and exposure times were used: 180 s in *B*, 2 × 120 s in *V* and 60 s in *R*. We chose the position of the AGN on the chip of DFOSC and the timing of the observations such that the bright star  $\epsilon$  Gru is off the chip and diffraction spikes are not affecting the AGN. The data were reduced using standard procedures in IRAF, using sky flats and bias frames taken at the end of the night. Photometric calibrations of the *B* and *V* data were performed using magnitudes of field stars from the AAVSO Photometric All-Sky Survey (APASS)<sup>2</sup> Data Release 6. To calibrate the *R* band we used a transformation of APASS Sloan *r'* and *i'* magnitudes to *R* following Jordi, Grebel & Ammon (2006). We find the following magnitudes:  $B = 15.55 \pm 0.07$ ,  $V = 15.45 \pm 0.05$  and  $R = 15.29 \pm 0.06$ , approximately equivalent to  $(3.9 \pm 0.3, 2.3 \pm 0.1, 1.46 \pm 0.08) \times 10^{-15} \text{ erg cm}^{-2} \text{ s}^{-1} \text{ \AA}^{-1}$ , respectively.

### 3 THE BLACK HOLE MASS

The optical spectra show strong emission lines from  $\text{H}\alpha$ ,  $\beta$ ,  $\gamma$ ,  $\delta$ , [O II], [O III], [N II] and [Ne III]. For this work we concentrate on the continuum and hydrogen line fits, in order to estimate the black hole mass. Optical spectral fitting was done with both the STARLINK DIPSO v3.6 spectral fitting package and IRAF. The continuum under

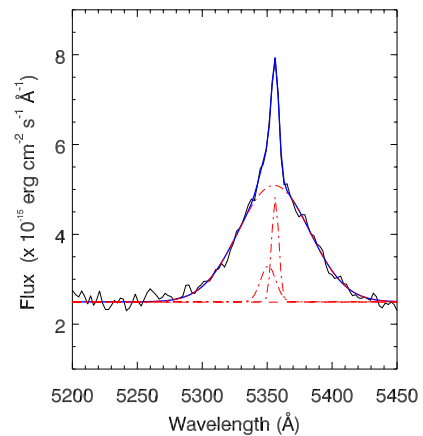


**Figure 1.** Fit to the observed  $\text{H}\beta$  profile during the 2000 October observations at SAAO.

each line was approximated by a first-order polynomial in the immediate vicinity of the line blend, Gaussian profiles were assumed for the line profiles and a least squares procedure was used to minimize the residuals of the fit. Both  $\text{H}\alpha$  and  $\text{H}\beta$  were best fitted with three Gaussians representing narrow, intermediate and broad components (e.g. Fig. 1). Towards the blue end of the spectrum the noise increased and the weaker broad lines of  $\text{H}\gamma$  and  $\text{H}\delta$  required only double and single Gaussian components, respectively. The positions of the line centres indicate a redshift of  $z = 0.1015 \pm 0.0010$ , consistent with the best published measurement of  $z = 0.1016 \pm 0.0001$  (Dunn et al. 2008).

We use the  $\text{H}\beta$  broad-line width (Table 2 and Fig. 1) together with either the luminosity from narrow-slit spectroscopy in 2000 October or the continuum flux at 5100 Å (rest frame) of  $1.36 \times 10^{-15} \text{ erg cm}^{-2} \text{ s}^{-1} \text{ \AA}^{-1}$  measured in the 2000 October 21/22

<sup>2</sup> <http://www.aavso.org/apass>

**Table 2.** H $\beta$  line fit in 2000 October, requiring three Gaussian components. All quantities are given in the observed frame, and errors are statistical only.

$\lambda_{\text{central}}$ (Å)	Amplitude (erg cm <sup>-2</sup> s <sup>-1</sup> Å <sup>-1</sup> )	FWHM (Å)	FWHM (km s <sup>-1</sup> )
5356.2 ± 0.2	(2.32 ± 0.23) × 10 <sup>-15</sup>	6.4 ± 0.7	358 ± 40
5350.8 ± 1.7	(8.03 ± 1.8) × 10 <sup>-16</sup>	13.7 ± 3.1	768 ± 174
5355.3 ± 0.5	(2.59 ± 0.06) × 10 <sup>-15</sup>	64.6 ± 0.9	3619 ± 51

wide-slit data to estimate the black hole mass. To convert flux to luminosity we used  $\Omega_M = 0.27$  and  $H_0 = 71$  km s<sup>-1</sup> Mpc<sup>-1</sup>. We follow the methods of Vestergaard & Peterson (2006, their section 3.4) for black hole mass estimation, with both equations resulting in estimates of  $\log M_{\text{BH}} = 8.1$ .

#### 4 SPECTRAL MODELLING

We combined the optical information with the X-ray data for our four quasi-simultaneous epochs. We removed the emission lines from the optical spectra and fitted the continua with a double power law which we use in the broad-band fits (e.g. Vanden Berk et al. 2001). All modelling is performed in the X-ray spectral fitting package XSPEC (Arnaud 1996). We use abundances from Wilms, Allen & McCray (2000) and the cross-sections of Verner et al. (1996). We fixed Galactic ( $z = 0$ ) X-ray absorption to  $9.43 \times 10^{19}$  cm<sup>-2</sup> (LAB H I Survey; Kalberla et al. 2005), and set reddening to  $1.7 \times N_{\text{H,Gal}}/10^{22}$  (Bessell 1991) as employed in J12a (and references therein). We note that  $N_{\text{H,Gal}}$  does not change significantly with respect to the LAB value when using the new method of Willingale et al. (2013), but is lower than the value of  $1.4 \times 10^{20}$  cm<sup>-2</sup> used in the earlier X-ray studies (Puchnarewicz et al. 1995; Breeveld et al. 2001).

For the epochs 2000 and 2001, we fitted the X-ray data with a simple absorbed power law plus blackbody model with all parameters excepting redshift and Galactic absorption free. This provided a good fit to the overall shape of the spectra, so a constant factor was included for the MOS spectra to determine the offsets between the XMM–Newton EPIC pn and MOS. These could then be fixed in more complex physical modelling to 1.09 (MOS1), 1.11 (MOS2) in 2000 and 1.06 (MOS1), 1.05 (MOS2) in 2001. The same procedure was carried out for the 2007 X-ray data, but a further two blackbodies were introduced in order to adequately reproduce the spectral shape: the Swift XRT spectrum did not require an offset, MOS1 was set to 1.02 and MOS2 to 1.01 with respect to pn. We did not allow offsets of the optical data with respect to the X-ray data. Clearly, a combination of multiple power laws and blackbodies is sufficient to describe the spectral shape at all epochs, but this is not a physically motivated model. We therefore go on to model each epoch in turn with more viable models for the emission mechanisms in AGN, which are necessarily more complex. All plots are shown in the observer frame.

##### 4.1 Epoch 2001

We began by modelling the SED taken in 2001, when the source flux was at its highest. The data at this epoch comprise XMM–Newton EPIC pn and MOS, and optical spectroscopy in the blue grating of the 1.9-m Radcliffe telescope.

We adopted the physical model *optxagnf* of D12. This comprises a colour–temperature corrected accretion disc spectrum with Comp-

tonization of both low temperature optically thick disc material and high temperature optically thin material in a corona. Black hole mass was fixed at  $10^{8.1} M_{\odot}$  from the H $\beta$  broad-line measurement (Section 3), and distance fixed at  $z = 0.1015$ , again as measured from the optical spectra. We also fixed the black hole spin to zero and outer disc radius to  $10^5 R_g$ . In addition to the fixed Galactic column, we allowed for an intrinsic absorber (*tbabs*; Wilms et al. 2000) and correlated reddening  $E(B - V)_{\text{int}} = 1.7 \times N_{\text{H,int}}/10^{22}$  (Bessell 1991).

Fitting this model to the data using  $\chi^2$  minimization we found the best-fitting power-law slope to be  $\Gamma = 1.87$ . The resulting black hole accretion rate was  $L/L_{\text{Edd}} = 0.27$  (resulting in  $\chi^2/\nu = 1172/1058$ ). The parameters resulting from this fit are very similar to those of one of the mean AGN spectra presented in J12a, Jin, Ward & Done (2012b) and D12 in which  $\langle M/M_{\odot} \rangle \sim 10^8$  and  $\langle L/L_{\text{Edd}} \rangle \sim 0.2$ . Our measured  $L/L_{\text{Edd}}$  is consistent with that measured by Grupe et al. (2010) from Swift data alone and using different models. Remarkably, no intrinsic absorption was required at all.

At energies above 2 keV, where our data are less constraining, this model assumes a pure power law. Many AGN are, however, well fitted with reflection off the disc above 2 keV, so we went on to include a reflection component with the *pexmon* XSPEC routine (Magdziarz & Zdziarski 1995). We assumed fixed solid angle  $\Omega/2\pi = 1$ , inclination angle  $30^\circ$  and  $\Gamma$  tied to the photon index of the disc+Comptonization model, using *rdblur* (based on Fabian et al. 1989) with  $R_{\text{in}} = 15 R_g$  to smear the Fe K $\alpha$  line since no narrow emission lines are apparent at this epoch. The total disc+Comptonization+reflection model is a good representation of the broad-band data ( $\chi^2/\nu = 1156/1058$ ), again with no measurable intrinsic neutral absorption. The power-law photon index steepens a little from  $\Gamma = 1.87$  to 2.07 when reflection is included, while the soft X-ray components and inferred accretion rate remain approximately the same ( $L/L_{\text{Edd}} = 0.25$ ). The Comptonization component responsible for the soft X-ray excess here is optically thick. Both models and their contributing components are shown in Fig. 2, and the data are shown with these models in Fig. 3. The best fits for both models are listed in Table 3. These can be compared with table 3 of D12, and appear to be similar to their mean AGN model M2.

We note that while we have no reason for allowing an offset between the optical and X-ray, if we do that no dramatic changes in the remaining free parameters are required and we obtain a comparable fit statistic. The optical constant factor goes to 0.8.

The distinction between these models lies primarily above a few tens of keV. The 15–50 keV Swift BAT data do not show any detection, even in the averaged flux considered for the BAT Survey (Baumgartner et al. 2013). The upper limit on its 70-month averaged flux is approximately 1 mCrab, which does not allow discrimination between these models. To extend the energy coverage towards the peak of the  $\nu F_{\nu}$  SED we overplotted the archival ROSAT Position Sensitive Proportional Counters (PSPC) spectrum (Puchnarewicz et al. 1995; Breeveld et al. 2001), and de-absorbed this according to the 2001 spectrum with extrapolation using our *optxagnf* model (Fig. 4). The soft X-ray spectrum in the PSPC data shows that the source had a strong soft excess in 1993 which is consistent with the 2001 data (it appears a little softer, which has been noted previously for PSPC spectra – see section 2.3.1 of Breeveld et al. 2001 for further details). We also estimated the approximate UV continuum flux in the IUE SWP (taken in 1992; Dunn et al. 2006) and combined FUSE (taken in 2002–2004; Dunn et al. 2010) observations using published spectra, and de-absorbed these using the LAB Survey Galactic value. Both are consistent with a UV spectrum rising to shorter wavelengths (within the 10 per cent errors we have assumed

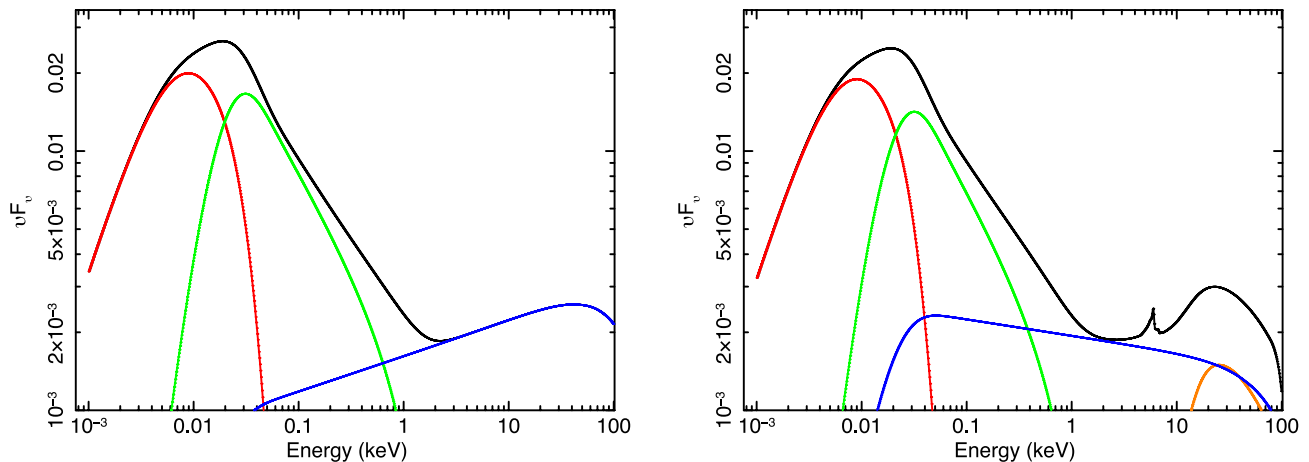


**Figure 2.** The colour–temperature corrected accretion disc plus Comptonization models (*optxagnf*, left) and including reflection (*optxagnf+rdblur\*pexmon*, right), which we applied to the SEDs. The black curves show the total unabsorbed model from the best fit to the epoch 2001 SED; red curves show the disc component; green curves show the soft X-ray Compton component; blue curves show the hard X-ray Compton component; the orange curve shows the *rdblur\*pexmon* reflection component (which includes an Fe line, visible here only in the total spectrum). The y-axis is in units  $\text{keV}^2 \text{ photons cm}^{-2} \text{ s}^{-1} \text{ keV}^{-1}$ .

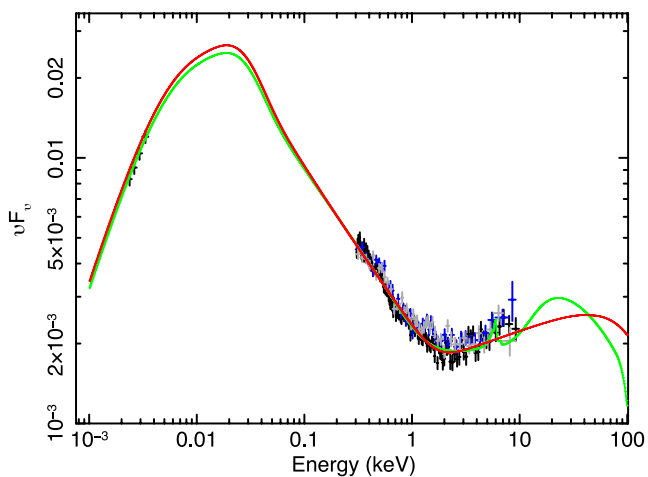


**Figure 3.** Unabsorbed SED at 2001 October (black points optical+pn, blue points MOS1, grey points MOS2), with the colour–temperature corrected accretion disc spectrum with Comptonization, *optxagnf* (red curve), and including reflection, *optxagnf+rdblur\*pexmon* (green curve). The y-axis is in units  $\text{keV}^2 \text{ photons cm}^{-2} \text{ s}^{-1} \text{ keV}^{-1}$  and energies are in the observer frame.

in Fig. 4), but we caution that source flux estimation in the UV is heavily absorption-model dependent.

We note that Puchnarewicz et al. (1995) performed SED fitting of the 1993 PSPC spectrum with the *ROSAT* Wide Field Camera (WFC) point and an optical spectrum taken 2 yr previously with the SAAO 1.9-m Radcliffe telescope, and also found an optical continuum rising to the blue and forming a big blue bump with the soft X-ray data.

Our model gives a monochromatic, unabsorbed luminosity at 200 eV of  $\log L(200) = 45.06$ , somewhat lower than the WFC luminosity of  $\log L(200) = 45.61$  (Edelson et al. 1999). Some of this discrepancy is due to the larger Galactic absorption column used ( $1.4 \times 10^{20}$  compared to our  $0.93 \times 10^{20} \text{ cm}^{-2}$ ; Edelson et al. 1999). However, this only increases our  $\log L(200)$  to 45.22, so there may be some intrinsic variability such that the source was brighter during the WFC survey than in our data set.

#### 4.2 Epoch 2000

The model parameters which describe the epoch 2001 SED are also a reasonable representation of the epoch 2000 SED (comprising EPIC pn, MOS1+2 and optical spectra), as shown in Fig. 5. We do, however, have a small flux deficit in optical and soft X-rays (Fig. 6), and this can be accounted for most simply by additional intrinsic X-ray absorption (using *tbabs*) of  $N_{\text{H}} = 1 \times 10^{20} \text{ cm}^{-2}$ , and additional intrinsic optical reddening of  $E(B - V) = 0.07 \text{ mag}$ . The resulting fit statistic for the *optxagnf* model is  $\chi^2/\nu = 1307/1071$ , and we note that to achieve this fit we untied the optical extinction and it converged at a value much greater than  $1.7 N_{\text{H}}$ . The key point here is that it is possible to keep the same continuum as seen in 2001, and change only the absorption to describe the 2000 SED. We also tried fixing all parameters but the power-law photon index and we obtain a good fit to the X-ray data with a flatter  $\Gamma = 1.81$ , while the optical data are still overpredicted by the model and additional reddening must be included.

#### 4.3 Epoch 2007

A simple overlay of the models adopted for the 2001 epoch is a poor description of the SED in 2007 (comprising EPIC pn, MOS1+2, *Swift* XRT and optical data), as can be seen in Fig. 7. An event must have occurred that suppressed both the bluest optical and soft X-ray flux, yet left the hard ( $> 5 \text{ keV}$ ) X-ray and redmost optical flux unaltered. The sharp features seen in residuals are strongly suggestive of absorption (Figs 6 and 7).

The 2007 *XMM-Newton* observation was the longest X-ray observation of RE J2248–511 with exposure of almost 60 ks. In these data an Fe line is detected, and fitting a Gaussian we measure an observed line centre of  $5.82 \pm 0.04 \text{ keV}$  (i.e. rest frame  $6.4 \text{ keV}$ ) and line width  $\sigma \leq 0.15 \text{ keV}$  as shown in Fig. 8. This leads us to prefer a model for the continuum which includes reflection.

Maintaining the same underlying disc+Comptonization+reflection continuum, and fitting for additional intrinsic neutral absorption (*tbabs*) and reddening ( $E(B - V)$ ) did not result in an acceptable fit and the SED shape was not well fitted ( $\chi^2/\nu = 147538/2049$ ). We then added a partial covering neutral absorber, *pcfabs*, and left  $E(B - V)$  and *tbabs*  $N_{\text{H}}$  at the source free to vary independently, and obtained a much improved fit. The resulting

**Table 3.** Overview of the best-fitting *optxagnf*+[*rdblur*\**pexmon*] SED model parameters for epoch 2001. Not listed are the fixed (frozen) parameters  $z = 0.1015$ ,  $M = 10^{8.1} M_{\odot}$ ,  $d_l = 462.1$  Mpc,  $N_{\text{H,Gal}} = 9.43 \times 10^{19} \text{ cm}^{-2}$ ,  $E(B - V)_{\text{Gal}} = 0.016 = 1.7 \times N_{\text{H,int}}/10^{22} \text{ mag}$ . The large number of free parameters relative to data points here makes obtaining explicit error bars on each parameter a difficulty, therefore, we do not present errors here but the uncertainties can be seen, in the broad sense, by comparison of the two models we have fitted.

Model	Parameter	Unit	<i>optxagnf</i>	<i>optxagnf</i> +[ <i>rdblur</i> * <i>pexmon</i> ]
<i>zTBabs</i>	$N_{\text{H}}$	$10^{20} \text{ cm}^{-2}$	0	0
<i>zredden</i>	$E(B - V)$	$=1.7 \frac{N_{\text{H}}}{10^{22}} \text{ mag}$	0	0
<i>rdblur</i>	Index	–	–	3 fixed
<i>rdblur</i>	$R_{\text{in}}$	$R_{\text{g}}$	–	15 fixed
<i>rdblur</i>	$R_{\text{out}}$	$R_{\text{g}}$	–	400 fixed
<i>rdblur</i>	Incl	deg	–	30 fixed
<i>pexmon</i>	$\Gamma^*$	–	–	2.07 <sup>a</sup>
<i>pexmon</i>	$E_{\text{fold}}$	keV	–	1000 fixed
<i>pexmon</i>	rel_refl	–	–	–1 fixed ( $ R  = 1$ )
<i>pexmon</i>	abund	–	–	1 fixed
<i>pexmon</i>	Fe_abund	–	–	1 fixed
<i>pexmon</i>	Incl	deg	–	30 fixed
<i>pexmon</i>	norm	–	–	0.002 fixed
<i>optxagnf</i>	$\log(L/L_{\text{Edd}})$	–	–0.57	–0.61
<i>optxagnf</i>	astar	–	0 fixed	0 fixed
<i>optxagnf</i>	$R_{\text{cor}}$	$R_{\text{g}}$	34	33
<i>optxagnf</i>	$\log(R_{\text{out}})$	$R_{\text{g}}$	5.0 fixed	5.0 fixed
<i>optxagnf</i>	$kT_e$	keV	0.28	0.21
<i>optxagnf</i>	$\tau$	–	13	15
<i>optxagnf</i>	$\Gamma$	–	1.87	2.07 <sup>a</sup>
<i>optxagnf</i>	$f_{\text{pl}}$	–	0.30	0.36
<i>optxagnf</i>	norm	–	1.0 fixed	1.0 fixed
	$\chi^2/\nu$	–	1172/1058	1156/1058

<sup>a</sup>The two photon indices were tied between *optxagnf* and *pexmon*.

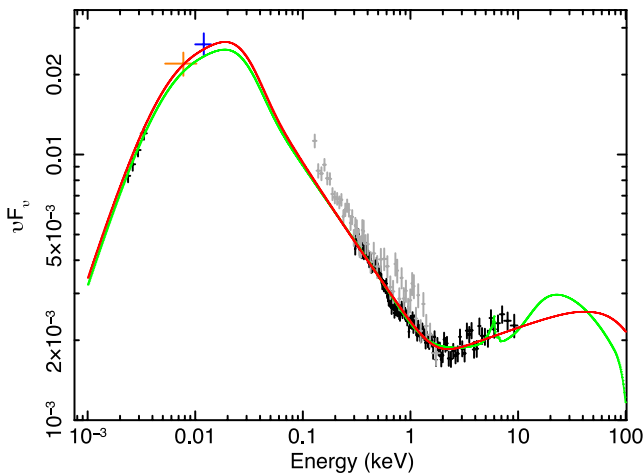


**Figure 4.** Unabsorbed SED at 2001 October (black points, showing optical and EPIC pn only for clarity), with the two possible models. We overplot the archival unabsorbed spectrum from *ROSAT* PSPC (grey) and the approximate continuum fluxes observed with *IUE* (orange) and *FUSE* (blue) assuming 10 per cent errors on each. The y-axis is in units  $\text{keV}^2 \text{ photons cm}^{-2} \text{ s}^{-1} \text{ keV}^{-1}$ .

partial covering column density required was  $N_{\text{H}} = 5.8 \times 10^{22} \text{ cm}^{-2}$  with covering fraction,  $f_{\text{cov}}$ , 0.4, and the neutral, fully covering absorbing column remained small (see Table 4). This was the simplest absorption model that could explain the large drop in optical to soft X-ray flux between 2001 and 2007, although it is likely that any absorption is far more complex in nature. Replacing the fully cov-

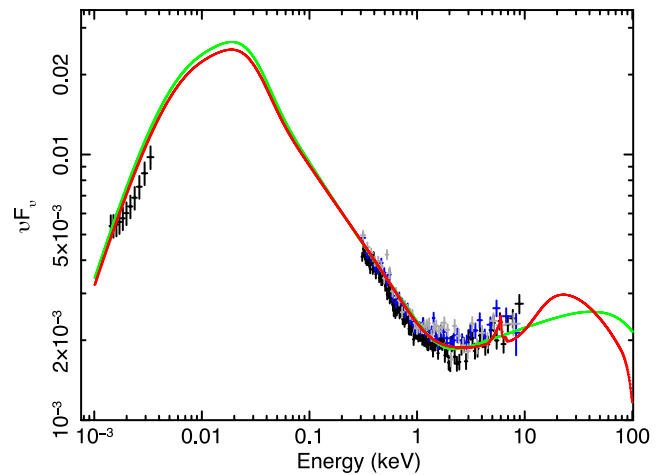


**Figure 5.** SED of October 2000 (black, blue and grey points for pn+optical, MOS1 and MOS2) with the epoch 2001 models overlaid (solid red and green lines as before). The y-axis is in units  $\text{keV}^2 \text{ photons cm}^{-2} \text{ s}^{-1} \text{ keV}^{-1}$ .

ering neutral absorber with an ionized absorber we found that the depth of the Fe unresolved transition array (e.g. Sako et al. 2001) was greatly overpredicted.

We examined data from the high resolution *XMM-Newton* Reflection Grating Spectrometer to shed further light on the details of the X-ray absorber. Unfortunately, there was insufficient signal to measure any spectral features.

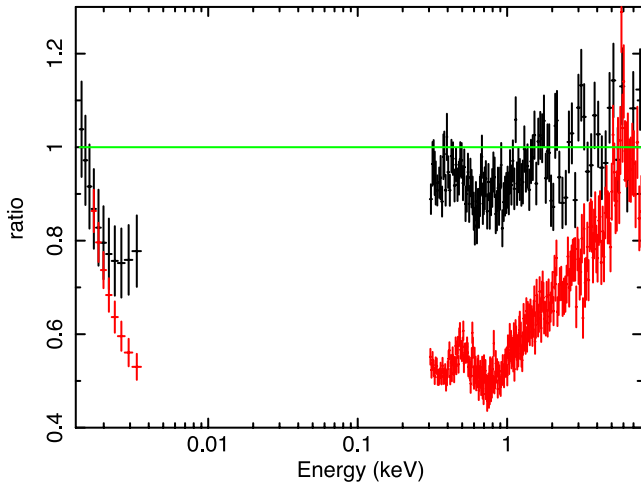


**Figure 6.** Ratio of the SEDs in October 2000 (black) and May 2007 (red) to the 2001 Model 1. For clarity we plot only the rebinned EPIC pn+optical data.

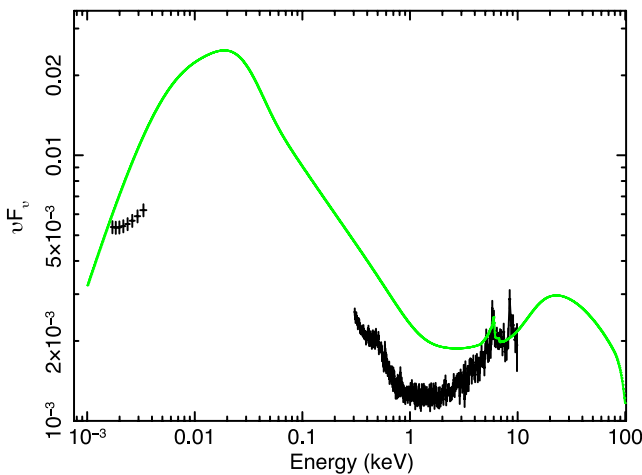


**Figure 7.** SED of May 2007 (black points) with the epoch 2001 *optxagnf+(rdblur\*pexmon)* model overlaid (solid green line). For clarity we plot only the rebinned EPIC pn+optical data and y-axis is in units  $\text{keV}^2 \text{ photons cm}^{-2} \text{ s}^{-1} \text{ keV}^{-1}$ .

#### 4.4 Epoch 2006

We fitted the 2006 September–November SED last because neither *XMM–Newton* data nor optical spectroscopy were available. The *Swift* XRT X-ray spectrum is similar in shape to that of 2007 with some small increase in flux (Fig. 9). We can therefore confirm that the strong X-ray absorption seen in 2007 was also present in 2006, to a lesser extent. The X-ray data are not of sufficient signal-to-noise ratio to discriminate between differing models, however, nor to extract details of either the continuum or the absorption model.

The optical photometry, reported in Section 2, includes a contribution from the emission lines. We estimated and removed the line contributions using previous optical spectra. The resulting *B*- and *V*-band fluxes are higher than measured in 2007 via spectroscopy, while the *R*-band flux is approximately the same. When plotted with the X-ray data in  $\nu F_\nu$  space the optical continuum shows little deviation from the 2001 model in contrast to the X-ray spectrum at this epoch (Fig. 9), but we caution that the errors may be underestimated if there are significant systematic uncertainties.

Finally, we overplotted the archival *ASCA* Gas Imaging Spectrometer (GIS) spectra (Breeveld et al. 2001) taken in 1997, and find that these lie between the 2001 and 2007 spectra examined here (Fig. 9).

#### 4.5 Long-term variability: summary of all epochs

These data allow the long-term spectral shape to be assessed at six epochs between 1992 and 2007. In 1993, the *ROSAT* spectrum agrees well with our model for the 2000 and 2001 data, as do the 1992 *IUE* and 2002–2004 average *FUSE* continua (with the caveat of strong absorption model dependency), suggesting the source was not significantly absorbed at these epochs. The *ASCA* spectra, taken in 1997, cover the portion of the spectrum dominated by Compton upscattering and reflection in our model. The fit residuals show a decline towards softer energies when compared with the 2001 model. In particular the lowest GIS energy bins covering 0.7–1.0 keV show 0.65–0.8 times the flux seen in 2001, but this is not conclusive and without coverage of soft X-ray or optical/UV regimes we cannot infer the presence or absence of absorption. In 2006 the XRT spectrum lies below the 2001 data, and we can infer that absorption is present when assuming the 2001 best-fitting model. In 2007 the XRT, EPIC and optical spectra show a large deficit in flux below 5 keV which we interpret as absorption.

## 5 DISCUSSION

The optical to X-ray SED of RE J2248–511 can be well represented by a colour–temperature corrected accretion disc spectrum with Comptonization of both low temperature optically thick disc material and high temperature optically thin material in a corona, plus a reflection component which is evident above 5 keV. In 2000–2001 little or no intrinsic absorption is required. The detection of this object in the FUV by the *ROSAT* WFC similarly requires that there was little or no intrinsic absorption at this epoch (1990) also.

However, the spectrum dramatically altered over the space of 5 yr in the soft X-ray and optical/UV, displaying a reduction in flux in both optical and X-ray, strongly suggestive of absorption. Indeed, additional fully and partially covering neutral absorbers plus additional reddening are able to explain the difference in SED shape seen in 2006–2007 whilst preserving the underlying continuum as seen in 2000–2001.

We know from detailed spectroscopic UV observations with *IUE*, *FUSE* and *Hubble Space Telescope (HST)* Cosmic Origins Spectrograph (COS) that complex absorbers exist in this system (Dunn et al. 2006, 2008, 2010; Borguet et al. 2012). These appear to lie at extremely large distances (9–15 kpc from the AGN), i.e. out into the halo of the host galaxy, so they possibly represent a galactic wind. Thus their density is extremely low, so they cannot vary in response to the changing illumination from the AGN, and indeed these are observed to remain constant.

The X-ray absorption we find here went unnoticed in the aforementioned work by Dunn et al. (2010). These authors looked only at the 2007 *XMM–Newton* spectrum, and were therefore unable to detect variability in the spectral shape and model any constant, underlying continuum. They concluded the X-ray spectrum was not absorbed, and compared this with the *FUSE* UV spectra taken in 2002 and 2004 which show evidence for significant absorption. From this they suggested that the source does not follow the 1:1 correspondence between UV and X-ray absorption claimed for low-redshift AGN (Crenshaw et al. 1999; Kriss 2006). Our findings

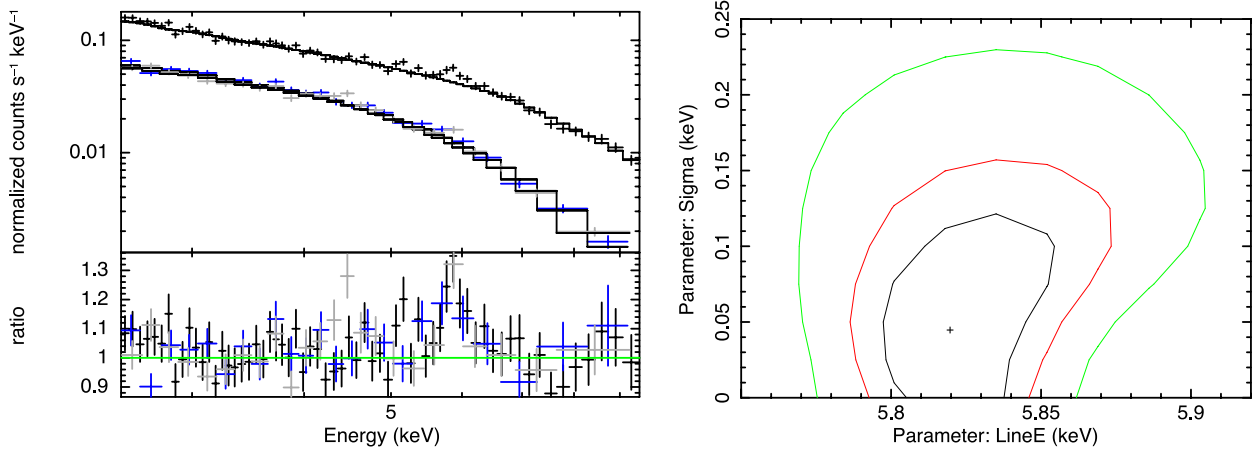


**Figure 8.** Left: data (upper panel) and data to model ratio (lower panel) for the 2.5–9.5 keV *XMM* data from 2007. A power-law model and the pn data are shown in black, MOS1 in blue and MOS2 in grey. An excess at the expected energy of an Fe line is apparent. Right: contour plot showing the 68, 90 and 99 percent confidence contours on the observed Gaussian line energy and width sigma.

**Table 4.** Intrinsic absorption required at epoch 2007, in addition to the *optxagnf*+(*rdblur*\**pexmon*) model parameters best-fitting at epoch 2001 (listed in Table 3).

Model	Parameter	Unit	Value
<i>zTBabs</i>	$N_{\text{H}}$	$10^{20} \text{ cm}^{-2}$	1.0
<i>zreddn</i>	$E(B - V)$	$= 1.7 \frac{N_{\text{H}}}{10^{22}} \text{ mag}$	0.11
<i>pcfabs</i>	$N_{\text{H}}$	$10^{22} \text{ cm}^{-2}$	5.8
<i>pcfabs</i>	$f_{\text{cov}}$		0.4
$\chi^2/\nu$			3038/2049

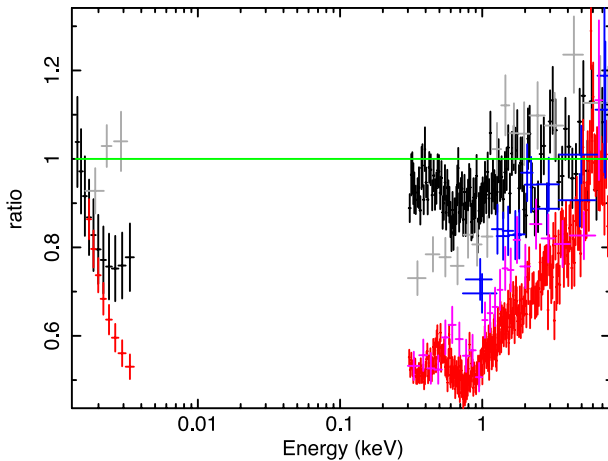


**Figure 9.** Ratio of the SEDs in 2000 October (black, pn+optical), 2007 May (red, pn+optical), 2007 September (pink, *Swift* XRT), 2006 September–November (grey, XRT+optical) and 1997 (blue, *ASCA* GIS) to the best-fitting 2001 *optxagnf* model.

show, however, that RE J2248–511 is strongly absorbed in the optical/UV to X-rays at some epochs and indeed these appear to be partially correlated.

A plausible scenario is that an absorbing cloud (system) crossed into our line-of-sight to the central AGN between 2005 and 2007, dramatically altering the optical to X-ray SED. The neutral X-ray absorber required an increase in column density of  $\sim 10^{20} \text{ cm}^{-2}$ ,

plus  $\sim 0.3$  mag of optical extinction ( $A_V$ ), while an additional 40 per cent partially covering X-ray absorber was invoked, with a large column of  $\sim 5 \times 10^{22} \text{ cm}^{-2}$  if neutral. This could be the onset of a new outflow, or a discrete episode of mass ejection. It is possible that a similar event occurred around 1997 as viewed by *ASCA* (Breeveld et al. 2001), or at least occurred sometime in between the epochs of 1993 and 2000 when strong soft excesses are clearly present; this is possibly also the case in 1992 when a flat optical continuum was noted (Mason et al. 1995) in contrast both to the bluer spectrum observed in 1991 (Grupe et al. 1998, 1999) and large soft X-ray excess seen with *ROSAT* in 1993 (Puchnarewicz et al. 1995, see also Breeveld et al. 2001).

To put RE J2248–511 in the wider context, we compare it to sources among the similarly analysed sample presented in J12a and Jin, Ward & Done 2012b,c. J12a took an X-ray/optically selected sample of unobscured *XMM*–SDSS Type I AGN, and modelled the SEDs with *optxagnf* as we have done here. Their sample contained 51 AGN, among which  $\sim 20$  per cent were NLS1. They concluded that these AGN could be carved up into three SED types and they reported the main parameters for each. The 2001 SED for RE J2248–511 is entirely consistent with their mean SED which has  $\langle M/M_{\odot} \rangle \sim 10^8$ ,  $\langle L/L_{\text{Edd}} \rangle \sim 0.2$ ,  $\langle R_{\text{cor}} \rangle \sim 40$ ,  $\langle kT_e \rangle \sim 0.3$ ,  $\langle \tau \rangle \sim 13$ ,  $\langle \Gamma \rangle \sim 1.87$  and  $\langle f_{\text{pl}} \rangle \sim 0.3$ . The Eddington fraction is perhaps the most likely parameter to be driving the spectral shape, and while NLS1s are around Eddington in most samples, we find a value of  $L/L_{\text{Edd}} \sim 0.25$ – $0.27$ , confirming RE J2248–511 as a typical BLS1s (e.g. Vasudevan & Fabian 2009; Grupe et al. 2010; J12a).

RE J2248–511 lies in a direction of low Galactic absorption. Combined with the total lack of measurable intrinsic absorption and reddening, this means we are seeing the AGN through a ‘hole’ in the Galactic and host galaxy column density. The continuum flux, which peaks at EUV energies, arrives uninhibited and as a consequence RE J2248–511 appears in EUV-selected samples. Given the very typical BLS1 continuum model parameters we obtain when fitting the non-absorbed epoch SEDs, this explanation is very attractive. This suggestion was originally made by Puchnarewicz et al. (1995), but with the potential for such dramatic changes caused by absorption alone, it is only with multi-epoch, multiwavelength data that we can now confirm this. The *ROSAT* WFC Extragalactic Survey AGN sample (Edelson et al. 1999) in which RE J2248–511 was catalogued, contains four to five AGN among the sample of 19

(including BL Lacs) with Galactic columns  $<10^{20}$  cm $^{-2}$ . The low intrinsic column and *ROSAT* WFC, *IUE* and *FUSE* detections show that there can be a high escape fraction for EUV and FUV photons from such AGN, which can be important for the AGN contribution to reionization of the Universe, both in terms of hydrogen and helium.

In summary, RE J2248–511 is a high black hole mass, broad-lined AGN in the local Universe, with an Eddington ratio similar to broad-lined quasars. Our modelling demonstrates that this spectral shape can be accommodated with a colour–temperature corrected accretion disc spectrum with Comptonization of both low temperature optically thick disc material and high temperature optically thin material in a corona, plus a reflection component. On time-scales of a few years the soft excess shows dramatic variability, which can be readily explained by the onset of absorption from both fully and partially covering material. We conclude that rather than an unusual, ultrasoft AGN which defies classification, RE J2248–511 is in fact a typical BLS1 that is fortuitously viewed through a ‘hole’ in the line-of-sight column density.

## ACKNOWLEDGEMENTS

RLCS acknowledges financial support from a Royal Society Dorothy Hodgkin Fellowship. We thank Jens Hjorth and Johan Fynbo for generously giving us observing time at the Danish Telescope, and Francois van Wyk for assistance during our first observing run at SAAO. We thank Hans Krimm and Wayne Baumgartner for assistance with the *Swift* BAT data, and Steve Sembay and Roberto Soria for useful discussions. KW acknowledges support from STFC. KLP acknowledges support from UKSA. This work is based on observations obtained with *XMM-Newton*, an ESA science mission with instruments and contributions directly funded by ESA Member States and the USA (NASA). This work made use of data supplied by the UK *Swift* Science Data Centre at the University of Leicester, and data provided by the High Energy Astrophysics Science Archive Research Center (HEASARC), which is a service of the Astrophysics Science Division at NASA/GSFC and the High Energy Astrophysics Division of the Smithsonian Astrophysical Observatory. This paper uses observations made at the South African Astronomical Observatory (SAAO). We acknowledge use of the AAVSO Photometric All-Sky Survey (APASS), funded by the Robert Martin Ayers Sciences Fund. Image Reduction and Analysis Facility (IRAF) is distributed by the National Optical Astronomy Observatories, which are operated by AURA, Inc., under cooperative agreement with the National Science Foundation.

We dedicate this work to the memory of Liz Puchnarewicz, who brought this source to the fore and inspired its further study.

## REFERENCES

Arnaud K. A., 1996, in Jacoby G. H., Barnes J., eds, ASP Conf. Ser. Vol. 101, *Astronomical Data Analysis Software and Systems V*. Astron. Soc. Pac., San Francisco, p. 17  
 Baumgartner W. H., Tueller J., Markwardt C. B., Skinner G. K., Barthelmy S., Mushotzky R. F., Evans P., Gehrels N., 2013, *ApJS*, 207, 19  
 Bessell M. S., 1991, *A&A*, 242, L17  
 Boller T. H., Brandt W. N., Fink H., 1996, *A&A*, 305, 53  
 Borguet B. C. J., Edmonds D., Arav N., Dunn J. P., Kriss G., 2012, *ApJ*, 751, 107  
 Boroson T. A., 2002, *ApJ*, 565, 78  
 Breeveld A. A., Puchnarewicz E. M., Otani C., 2001, *MNRAS*, 325, 772

Brocksopp C., Starling R. L. C., Schady P., Mason K. O., Romero-Colmenero E., Puchnarewicz E. M., 2006, *MNRAS*, 366, 953  
 Burrows D. et al., 2005, *Space Sci. Rev.*, 120, 165  
 Collin S., Kawaguchi T., Peterson B. M., Vestergaard M., 2006, *A&A*, 456, 75  
 Crenshaw D. M., Kraemer S. B., Boggess A., Maran S. P., Mushotzky R. F., Wu C.-C., 1999, *ApJ*, 516, 750  
 Crummy J., Fabian A. C., Gallo L., Ross R. R., 2006, *MNRAS*, 365, 1067  
 Czerny B., Nikolajuk M., Róźańska A., Dumont A.-M., Loska Z., Zycki P. T., 2003, *A&A*, 412, 317  
 Done C., Nayakshin S., 2007, *MNRAS*, 377, L59  
 Done C., Davis S. W., Jin C., Blaes O., Ward M., 2012, *MNRAS*, 420, 1848 (D12)  
 Done C., Jin C., Middleton M. J., Ward M., 2013, *MNRAS*, 434, 1955  
 Dultzin D., Martínez M. L., Marziani P., Sulentic J. W., Negrete A., 2011, in Foschini L., Colpi M., Gallo L., Grupe D., Komossa S., Leighly K., Mathur S., eds, *Proc. of Narrow-Line Seyfert 1 Galaxies and Their Place in the Universe*. PoS, Milano, Italy, p. 12  
 Dunn J. P., Jackson B., Deo R. P., Farrington C., Das V., Crenshaw D. M., 2006, *PASP*, 118, 572  
 Dunn J. P., Crenshaw D. M., Kraemer S. B., Trippe M. L., 2008, *AJ*, 136, 1201  
 Dunn J. P., Crenshaw D. M., Kraemer S. B., Trippe M. L., 2010, *ApJ*, 713, 900  
 Edelson R., Vaughan S., Warwick R., Puchnarewicz E., George I., 1999, *MNRAS*, 307, 91  
 Elvis M. et al., 1994, *ApJS*, 95, 1  
 Evans P. A. et al., 2009, *MNRAS*, 397, 1177  
 Fabian A. C., Rees M. J., Stella L., White N. E., 1989, *MNRAS*, 238, 729  
 Fabian A. C. et al., 2009, *Nature*, 459, 540  
 Fabian A. C. et al., 2013, *MNRAS*, 429, 2917  
 Gallo L. C., 2006, *MNRAS*, 368, 479  
 Gehrels N. et al., 2004, *ApJ*, 611, 1005  
 Gierliński M., Done C., 2004, *MNRAS*, 349, L7  
 Grupe D., Beuermann K., Thomas H.-C., Mannheim K., Fink H. H., 1998, *A&A*, 330, 25  
 Grupe D., Beuermann K., Mannheim K., Thomas H.-C., 1999, *A&A*, 350, 805  
 Grupe D., Komossa S., Leighly K. M., Page K. L., 2010, *ApJS*, 187, 64  
 Jansen F. et al., 2001, *A&A*, 365, L1  
 Jin C., Done C., Ward M., Gierliński M., Mullaney J., 2009, *MNRAS*, 398, L16  
 Jin C., Ward M., Done C., Gelbord J., 2012a, *MNRAS*, 420, 1825 (J12a)  
 Jin C., Ward M., Done C., 2012b, *MNRAS*, 422, 3268  
 Jin C., Ward M., Done C., 2012c, *MNRAS*, 425, 907  
 Jin C., Done C., Middleton M., Ward M., 2013, *MNRAS*, preprint (arXiv:1309.5875)  
 Jordi K., Grebel E. K., Ammon K., 2006, *A&A*, 460, 339  
 Kalberla P. M. W., Burton W. B., Hartmann D., Arnal E. M., Bajaja E., Morras R., Pöppel W. G. L., 2005, *A&A*, 440, 775  
 Kriss G. A., 2006, in Sonneborn G., Moos H., Andersson B.-G., eds, *ASP Conf. Ser. Vol. 348, Astrophysics in the Far Ultraviolet: Five Years of Discovery with FUSE*. Astron. Soc. Pac., San Francisco, p. 499  
 Laor A., Fiore F., Elvis M., Wilkes B. J., McDowell J. C., 1997, *ApJ*, 477, 93  
 Lohfink A. M., Reynolds C. S., Mushotzky R. F., Nowak M. A., 2013, *Mem. Soc. Astron. Ital.*, 84, 1  
 Magdziarz P., Zdziarski A., 1995, *MNRAS*, 273, 837  
 Magdziarz P., Blaes O. M., Zdziarski A. A., Johnson W. N., Smith D. A., 1998, *MNRAS*, 301, 179  
 Mason K. O. et al., 1995, *MNRAS*, 274, 1194  
 Mehdipour M. et al., 2011, *A&A*, 534, 39  
 Middleton M., Done C., Gierliński M., 2007, *MNRAS*, 381, 1426  
 Middleton M., Done C., Ward M., Gierliński M., Schurch N., 2009, *MNRAS*, 394, 250  
 Noda H., Makishima K., Yamada S., Torii S., Sakurai S., Nakazawa K., 2011, *PASJ*, 63, S925

- Noda H., Makishima K., Nakazawa K., Uchiyama H., Yamada S., Sakurai S., 2013, *PASJ*, 65, 4
- Osterbrock D. E., Pogge R. W., 1985, *ApJ*, 297, 166
- Peterson B. M., 2011, in Foschini L., Colpi M., Gallo L., Grupe D., Komossa S., Leighly K., Mathur S., eds, *Narrow-Line Seyfert 1 Galaxies and Their Place in the Universe*. PoS, Milano, Italy, p. 32
- Pounds K. A. et al., 1993, *MNRAS*, 260, 77
- Puchnarewicz E. M., Branduardi-Raymont G., Mason K. O., Sekiguchi K., 1995, *MNRAS*, 276, 1281
- Sako M. et al., 2001, *A&A*, 365, L168
- Schurch N. J., Done C., 2007, *MNRAS*, 381, 1413
- Shakura N. I., Sunyaev R. A., 1973, *A&A*, 24, 337
- Strüder L. et al., 2001, *A&A*, 365, L18
- Sulentic J. W., Marziani P., Dultzin-Hacyan D., 2000, *ARA&A*, 38, 521
- Vanden Berk D. E. et al., 2001, *AJ*, 122, 549
- Vasudevan R. V., Fabian A. C., 2007, *MNRAS*, 381, 1235
- Vasudevan R. V., Fabian A. C., 2009, *MNRAS*, 392, 1124
- Verner D. A., Ferland G. J., Korista K. T., Yakovlev D. G., 1996, *ApJ*, 465, 487
- Vestergaard M., Peterson B. M., 2006, *ApJ*, 641, 689
- Walton D. J., Nardini E., Fabian A. C., Gallo L. C., Reis R. C., 2013, *MNRAS*, 428, 2901
- Wilkes B. J., Elvis M., McHardy I., 1987, *ApJ*, 321, L23
- Willingale R., Starling R. L. C., Beardmore A. P., Tanvir N. R., O'Brien P. T., 2013, *MNRAS*, 431, 394
- Wilms J., Allen A., McCray R., 2000, *ApJ*, 542, 914

This paper has been typeset from a  $\text{\TeX}/\text{\LaTeX}$  file prepared by the author.